Int. J. Electrochem. Sci., 14 **(2019)** 6195 – 6208, doi: 10.20964/2019.07.47

International Journal of
ELECTROCHEMICAL
SCIENCE
www.electrochemsci.org

Developing a point-of-care System for Determination of Dopamine, Ascorbic and Uric Acids in Biological Fluids Using a Screen-Printed Electrode Modified by Three Dimensional Graphene/Carbon Nanotube Hybrid

Ali Farahani, Hassan Sereshti[*]

School of Chemistry, College of Science, University of Tehran, Tehran, Iran
[*]E-mail: sereshti@ut.ac.ir

Received: 10 January 2019 / *Accepted:* 11 March 2019 / *Published:* 10 June 2019

A cost-effective point-of-care (POC) device including a potentiostat, a modified screen printed electrode (SPE) placed in a custom-designed microfluidic chamber, and a homemade syringe pump setup was developed as an electrochemical assay for determination of dopamine (DA), ascorbic acid (AA), and uric acid (UA) in human plasma and urine. SPE was modified with three-dimensional graphene/carbon nanotube (3DG/CNT) used as a new electrochemical sensor. A microcontroller-based potentiostat was developed to perform cyclic voltammetry (CV) and differential pulse voltammetry (DPV) measurements. The syringe pump system based on open source electronics was made to guide the solution through a microfluidic chamber. In order to improve the quantification accuracy, the DPV peaks were resolved, using partial least square (PLS) method. The detection limits were AA (2.5 µM), DA (0.4 µM), and UA (0.6 µM) (signal to noise ratio, 3). The linear dynamic ranges were 4-2000, 0.5-2000, and 0.8-1500 µM for DA, AA, and UA, respectively. The precision of the method (RSD, n=3) was < 2.2 %.

Keywords: Biomedical diagnostic; Dopamine; Electroanalytical chemistry; Modified screen-printed electrode; Three dimensional structure nanomaterials;

1. INTRODUCTION

The development of cost effective and portable miniaturized platform or point-of-care (POC) systems is a main subject within the primary healthcare. In POCs all tests can be performed close to the patient [1]. Compared with traditional laboratory testing with large instruments, which are labor-intensive, time-consuming and expensive, POC testing is sensitive, affordable, rapid, specific, user-friendly, equipment-free, robust and deliverable to end users [2,3]. The microfluidics-based biosensors have attracted the attention of researchers because of their potential applications in global health, food safety, personalized medicine, drug discovery clinical diagnostics, and forensics. The request for

biosensors and bioelectronics capable of detecting biological warfare agents has increased, and the research is focused on ways of producing miniature portable devices that would allow rapid, accurate, and on-the-spot detection [4]. Dopamine (DA) is a major neurotransmitter that has a critical role in the mammalian focal nervous system for message transfer. Moreover, it is implicated in the pathogeneses and treatment of a variety of psychiatric disorders and the regulation of cognitive functions. Therefore, quantitative measurement of DA is essential. Since DA is electroactive catecholamine, thus its electrochemical detection with the advantages such as speed, simplicity, and sensitivity is preferred. Between many methods for detection of DA in biological samples, voltammetric method has shown to be a powerful tool. However, the principal challenge in the electrochemical determination of DA is the coexistence of other biologically significant compounds such as ascorbic acid (AA) and uric acid (UA) at a higher concentration than DA exists [5]. Moreover, these compounds are also oxidized at a potential near to DA, which results in the overlapping of electrochemical response. UA is the main final product of purine metabolism, and it is one of the main biomolecules present in urine and blood. Elevated UA levels in the urine may be a sign of spreading cancer, Lesch–Nyhan syndrome, consumption of a purine-rich diet gout, Fanconi syndrome and rhabdomyolysis. AA is also one of the main components in the human diet, and it plays an essential role in bioelectrochemistry, neurochemistry, and clinical diagnostics applications. It has been also used for the prevention and treatment of mental illness, scurvy, and cancer which is very important [6,7].

Generally, the redox reactions of such species at unmodified electrodes suffer from irreversibility, electrochemical detections at high overpotentials [8], and very similar potentials, and pronounced fouling effect [9]. In order to the simultaneous determination of AA, DA and UA, different materials such as metal complexes, polymers and carbon materials have been used to modify electrodes. Between them, carbon-based nanomaterials such as graphene (G) and carbon nanotubes (CNTs) are the most frequently used modifiers, because of their large electrochemical active surface area and good catalytic activity [10-14]. However, due to the π–π stacking, hydrophobic interactions, and van der Waals forces between individual G sheets, it tends to form irreversible agglomeration or even restock to form graphite. This may also significantly decrease the high specific surface area of G, which is unfavored for its applications. To solve this problem, the G sheets can be reassembled into three-dimensional graphene (3DG) structures. Compared with 2D-G, the 3D structures have higher specific surface area, stronger mechanical strength, lower density, and faster mass and electron transport kinetics due to combining 3D interconnected framework and excellent intrinsic properties of G. The ultrahigh surface area, hollow structure, porosity, and fast mass transport kinetics of 3DG make it a promising candidate for modifying electrode surface [15]. Moreover, the addition of CNTs can bridge adjoin G to reduce their aggregation efficiently. In addition, electrodes modified only with CNTs or G alone cannot determine AA, DA and UA selectively, so it is intransitive to functionalize carbon materials [14].

In this research, a POC device consisting of a modified SPE electrode in a microfluidic chamber connected with a syringe pump assembly and a miniature potentiostat was developed for the first time. The 3DG/CNTs network was successfully fabricated on the surface of SPE by electrodeposition method. The device was utilized for determination of DA, AA, and UA in biological samples through CV and DPV measurements. In order to enhance sensitivity and resolve overlapping peaks, partial least square technique was applied to the electrochemical response.

2. EXPERIMENTAL

2.1 Materials and reagents

Ascorbic acid, dopamine, uric acid and lithium perchlorate ($LiClO_4$) were purchased from Sigma Aldrich (St. Luis, MO, USA). Graphite powder (300 mesh, spectral pure) was obtained from Merck Chemicals (Darmstadt, Germany). A phosphate buffer solution (PBS, 0.1 M, pH 7.0) was prepared using Na_2HPO_4 and NaH_2PO_4 and used as supporting electrolyte. The chemicals and reagents with analytical grade and used without further purification.

2.2 Equipments

The cyclic voltammetry (CV) and differential pulse voltammetry (DPV) measurements were performed with the developed POC device. The bare SPE electrode was obtained from Metrohm AG (Herisau, Switzerland). The impedance data were fitted to equivalent circuit using Zview 3.0 software. An Ivium Palmsens 2 (Houten, Netherland) was used to validate the performance of the designed potentiostat. The electrochemical impedance spectroscopy measurements were taken with a CHI 660 electrochemical workstation (CH Instruments, Austin, TX, USA). The electrochemical cell, which used for primary test consisted of glassy carbon electrode (GCE, 3 mm, Bioanalytical Systems, Inc., Beijing, China) as the working electrode, a platinum wire as the counter electrode and Ag/AgCl Metrohm AG (Herisau, Switzerland) as the reference electrode. The Raman spectrum were obtained utilizing a Thermo Nicolet XR Raman Spectrometer (MA, USA).

2.3 The point-of-care analyzer

The developed POC device was made of three main parts including a microfluidic chamber, a potentiostat, and a syringe pump assembly (Fig. 1).

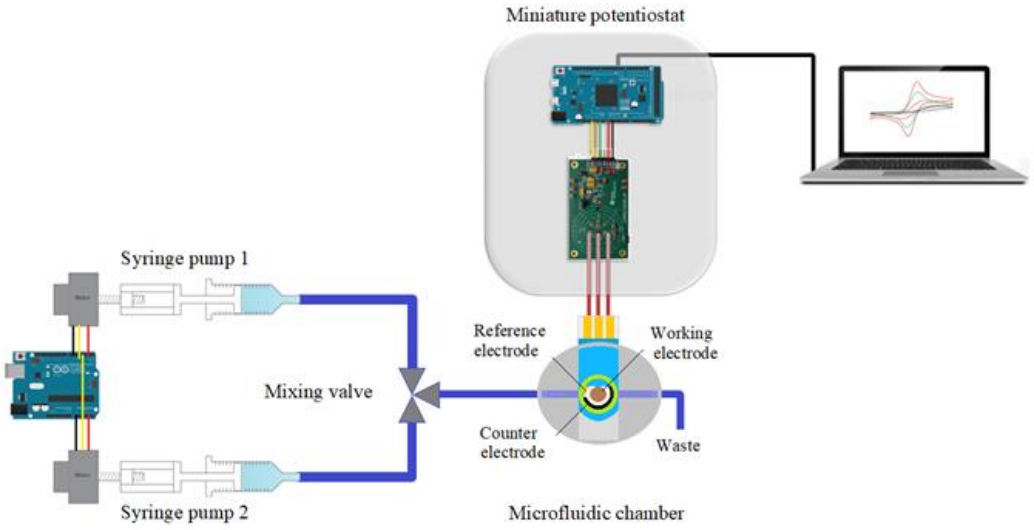

Figure 1. The main components of the developed point-of-care system.

a) Microfluidic chamber. A homemade microfluidic chamber was designed to fit the modified 3DG/CNT-SPE electrode for performing electrochemical measurements. The chamber was placed after a syringe pump assembly that provides precise and repeatable volume. A mixing valve merges the sample and buffer solutions flows, and brings the mixture to the chamber through a polyethylene tube (i.d., 0.8 mm). The electrode has been placed between two polydimethylsiloxane blocks of the microfluidic chamber. The lower block of the chamber includes appropriate margins to position an O-ring to seal the upper SPE surface.

b) The potentiostat. This part consists of a modified gas sensor (LMP91000, Texas instrument, USA) (Fig. 2) and a microcontroller (Arduino, Italy). The sensor was reconfigured to perform CV and DPV measurements. An Arduino Due based on 84 MHz ARM microcontroller was added to the system instead of the commonly used and expensive field programmable gate array (FPGA) board. The sensor was powered and controlled via an I^2C interface.

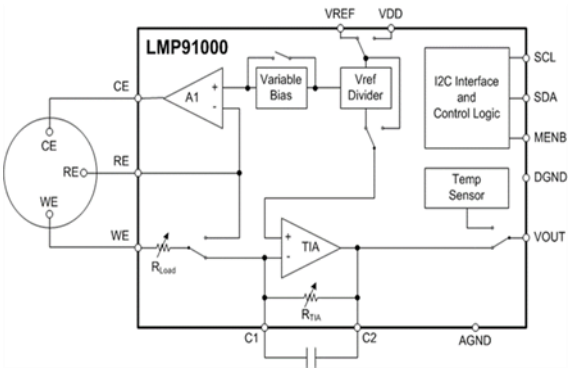

Figure 2. The new configuration for LMP91000-EVM for electrochemical measurements. The ADC unit transfers data to Arduino via an SPI protocol.

The measurements were validated using two commercial potentiostats (Palmsens 2 & EMstat) for Fe(II)/Fe(III) redox in PBS buffer (Fig. 3). The results indicate that the difference between the peaks is not significant.

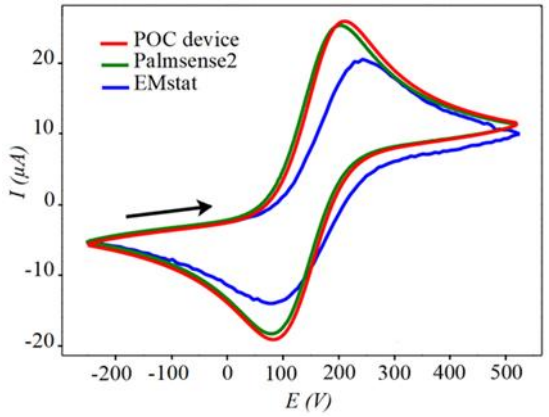

Figure 3. Comparison between cyclic voltammograms of $Fe(CN)_6^{4-}$ (10^{-4} M in 0.1 M PBS) obtained from two commercial potentiostats (Palmsense2 & EMstat) and the developed POC system.

Syringe pump. Two low-cost, miniaturized syringe pump for precise infusion and withdrawal of sample solutions was made using (Arduino Uno) open source instrument hardware and 3D printer build-parts. The pumps are programmed and controlled by Arduino user interface and DRV8825, stepper motor driver.

2.4 Synthesis procedure.

The reduced-GO nanosheets were synthesized using graphite powder by a modified Hummer method [16]. The 3DG network was prepared through electrodeposition of GO sheets on the SPE surface. Briefly, 0.15 g of GO and 0.01 g CNT were added to a 0.1 M water solution of $LiClO_4$ and sonicated for 15 min. The electrodeposition of the mixture (GO/CNT) was carried out with the CV method (conditions: the potential range, zero to -1.5 V; scan rate, 100 mV s^{-1}; and cycles, 10). To remove unreacted materials, the modified electrode was washed with deionized water. Then, it was freeze-dried to fix the 3D structure. Cathodic potential of −1.2 V were applied for 5 min, the porous 3DG structure was immobilized on the surface of electrode.

2.5 Electrochemical modification of electrode surface

Different methods have been offered for fabrication of 3DG-based compositions including template-directed chemical vapor deposition [17], hydrothermal reduction [18], gelation of graphene oxide [19], and electrochemical reduction [20]. Among these techniques, electrochemical reduction is an echo-friendly, easy, and inexpensive method. In addition, it is the most suitable approach for modification of electrode surface, because reduced graphene sheets can be directly deposited on the surface of electrodes [20]. Therefore, in this study, the surface of the SPE electrode was modified with 3DG/CNT to improve the sensitivity. Carbon nanotubes (CNTs) was also added to prevent aggregation of graphene nanosheets. The CNTs also act as nanowires to improve the surface electrical conductivity (Fig. 4).

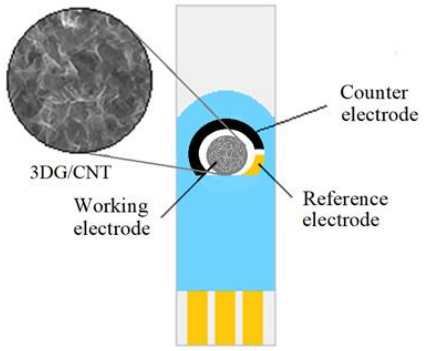

Figure 4. The schematic of 3DG/CNT-SPE electrode.

2.6 Data processing

The PLS is a multiple linear regression technique that can resolve data with strongly associated, noisy, and a large number of *X*-variables, and simultaneously build models for several response variables [21]. It decomposes *X* and *Y* matrices into score and loading matrices using singular value decomposition algorithm and then maximizes the covariance between scores in *X* and *Y* spaces. It can simply describe the *Y* matrix in the directions, which are the most correlated to the *X* matrix. Using PLS technique overlapped signals were resolved and wider linear range and lower limit of detection were observed. In recent researches for determination of neurotransmitters most of the time the modifiers not only enhance the sensitivity but also improve the separation of peaks that is the influence of different kinetics of analytes on the surface of electrode, which lead to simultaneous determination of target analytes [22]. In this study, the modifier only enhances the peak current of analytes, which means a better sensitivity is achievable, but it seems that the kinetic of analytes is not that much different on the surface of modified electrode therefore the resolution of peaks is not sufficient for simultaneous determination here is the critical point, which PLS is used. The technique is capable of resolving overlapped peaks [23-25]. As we searched through there is no reports of using such techniques in combination with electrochemical techniques for simultaneous determination of target analytes. The MATLAB & Simulink R2016b software were used for data modeling and coding, respectively.

3. RESULTS AND DISCUSSION

3.1 Structural and electrochemical characterization

Figures 5a and 5b shows the SEM micrographs of the modified 3DG/CNT-SPE electrode after electrodeposition of reduced-GO and CNT on the surface of SPE. As it is obvious, the reduced graphene sheets and CNTs have been randomly connected with each other to form a macroscopic porous and cavity-like 3D structure. The 3D structure facilitates the access of analytes to high electrode surface. The pore walls contain oriented graphene sheets with exposed active sites that catalyze the redox reactions on the surface of the electrode for electron transfer. Moreover, the electrodeposition time has a great effect on composition of 3D structure. At the times shorter than 300 s, poor 3D structure was observed. The Raman spectra of 3DG and 3DG/CNT in Fig. 5c displays 2 main peaks at ~1360 and 1650 cm^{-1}, which could be ascribed to band of D and G for graphene sheets, respectively. The G band results from in-plane vibrations of sp^2 bonded carbon atoms while the D band is because of out-of-plane vibrations ascribed to the presence of structural deficiency [26]. The intensity of D/G ratio in the Raman spectrum of GO is approximately equal to 0.45. However, after electrodeposition of 3DG/CNT on the SPE electrode, the D/G ratio increased to 0.67, which demonstrates the resumption of sp^2 conjugation in the graphite structures [16]. Moreover, the appearance of a 2D band (at ~2500 cm^{-1}) displays the successful concatenation of CNTs to the 3DG structure. The single layer graphene can also be identified by analysis of the 2D/G ratio. As can be seen in Fig. 5c the 2D/G ratio of 3DG/CNT has significantly been enhanced compared to that of 3DG [27]. Therefore, the incorporation of CNTs led to the formation of single-layer graphene with the higher surface area.

The kinetics of electron transfer in a redox system at the 3DG/CNT-SPE electrode and an SPE electrode surface was compared based on impedance measurements (Fig. 5d). The resistance of charge transfer (R_{ct}) value for the redox system was calculated as the diameter of the high-frequency half-circle in the Nyquist plots. By fitting the data, R_{ct} at the 3DG/CNT-SPE was smaller than that obtained at the SPE electrode. Enhancement in the kinetics of electron transfer can be attributed to the presence of 3DG/CNT. The equivalency circuit and slope of Warburg also confirm the faster kinetic of electron transfer in modified electrode [28].

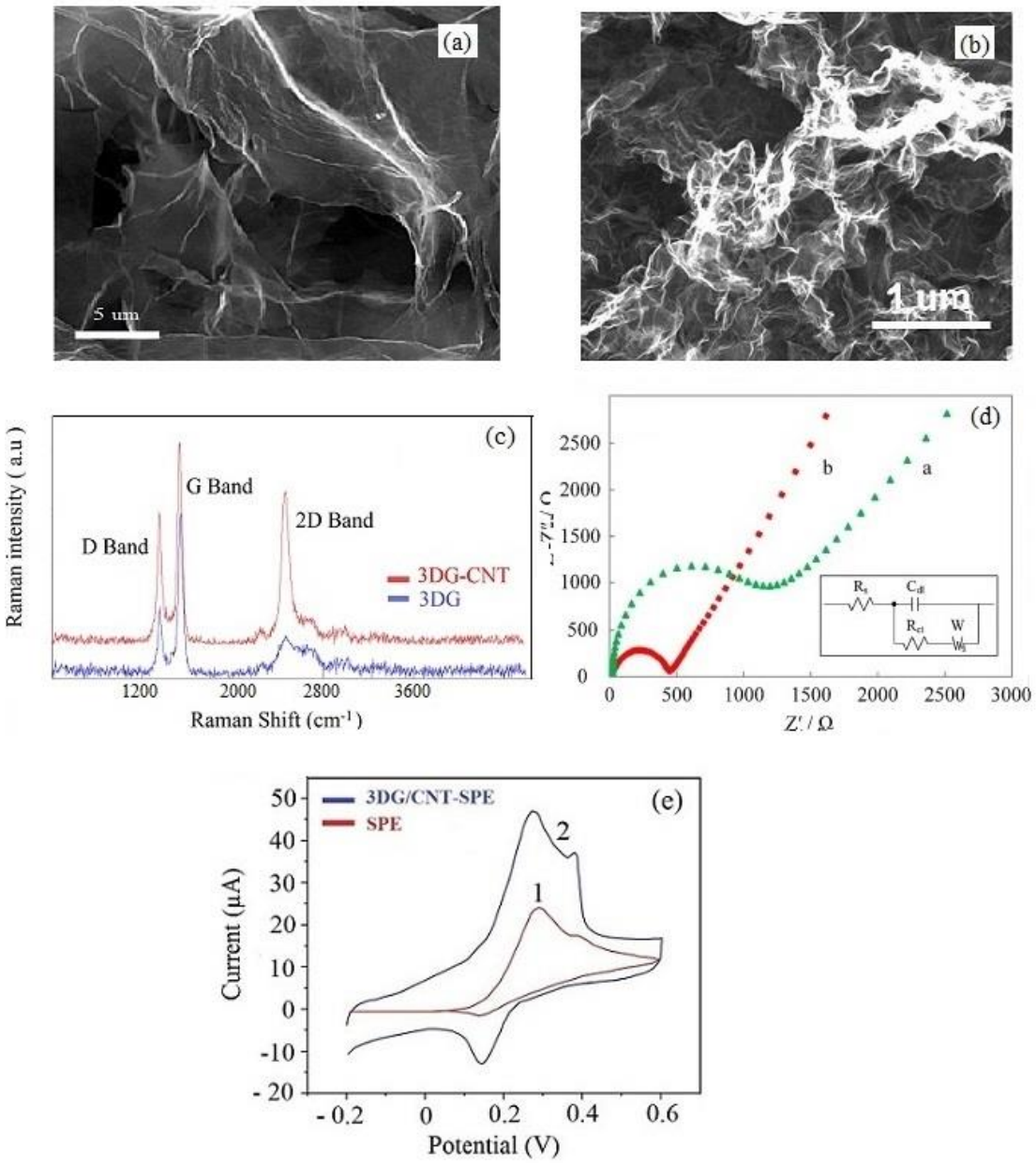

Figure 5. (a) and (b) The SEM micrographs of synthesized 3DG network. (c) The Raman spectra of 3DG and 3DG/CNT. (d) The impedance plots of (a) the SPE; and (b) 3DG/CNT-SPE in 10^{-1} M KCl solution containing 5×10^{-3}M $Fe(CN)_6^{4-}$ and inset is equivalent circuit. (e) Cyclic volammograms of (1) SPE electrode, (2) and 3DG/CNT-SPE in phosphate buffer solution (pH 7) containing 10^{-3} M ascorbic acid, uric acid, and dopamine.

The sensing efficiency of SPE and 3DG/CNT-SPE electrodes for determination of AA, UA and DA was compared under the same experimental conditions (PBS (pH 7) containing 10^{-3} M AA, UA and DA. Figure 5e shows the cyclic voltammograms of the AA, UA and DA mixture. The faradic current obtained with the 3DG/CNT-SPE electrode is remarkably higher than that of the SPE electrode. This leads to an improved sensitivity and detection limit. Moreover, 3DG/CNT-SPE shows a sharper peak with a negative shift, which indicates a faster electron transfer compared with SPE electrode. Therefore, 3DG/CNT-SPE electrode was more suitable for sensing target analytes in the subsequent experiments.

3.2 Effect of scan rate

In cyclic voltammetry, scanning the potential in negative and positive directions provide to explore the electrochemical behavior of the target electroactive analyte at the electrode. Therefore, the influence of this parameter was investigated in range of 20-500 mV/s. Figure 6a shows a linear relationship between the oxidation current and the scan rate (20-100 mV/s). This indicates a surface controlled mechanism. At higher scan rates Figure 6b (200-500 mV/s) the linearity between the peak current and the square root of the scan rate indicates that the electrooxidation is controlled by diffusion of active species. The change of mechanism from surface control to diffusion control at higher scan rates leads to a faster electron transfer at the 3DG/CNT-SPE electrode compared with unmodified SPE electrode [29]. Additionally, as scan rate increase, a positive shift is observed for three analytes.

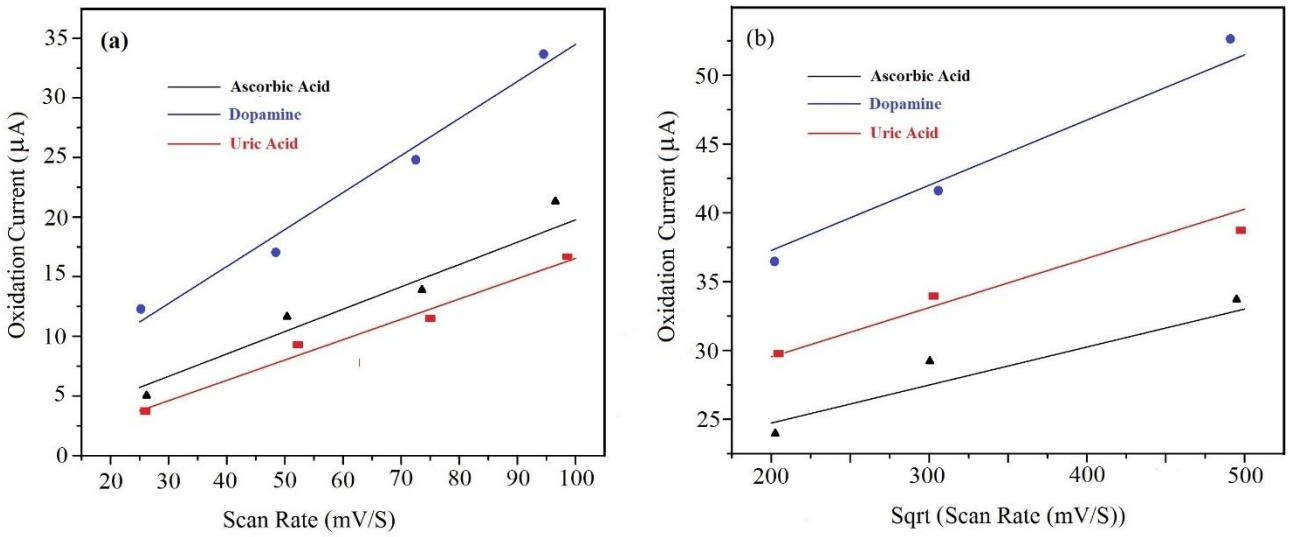

Figure 6. Cyclic voltammetric response of 5×10^{-4} M ascorbic acid, dopamine and uric acid using the 3DG/CNT-SPE electrode at 25, 50, 75, 100, 200, 300 and 500 mV s^{-1} scan rates using the developed POC device.; (a) the linear relationship between scan rate and peak current; (b) the linear relationship between scan rate and square root. All sample solution was prepared in PBS (10^{-4} M).

3.3 Effect of pH

In most cases, it is important to study the effect of pH on electrochemical behavior of analytes. Therefore, differential pulse voltammograms of a standard solution of AA, DA and UA (6×10^{-4} M) mixture were recorded at different pH values of phosphate buffer solution (4-8). As shown in Fig. 7 due to overlapping the signals the maximum peak current was used as a measure for optimizing. As pH increases from 4 to 7, the peaks shifted to more negative values and the peak current increased gradually and after that decreased. This can be attributed to the participation of H^+ ions in electrochemical reaction on the surface of electrode [30]. Therefore, the pH 7 was used for all experiments measuring AA, DA and UA.

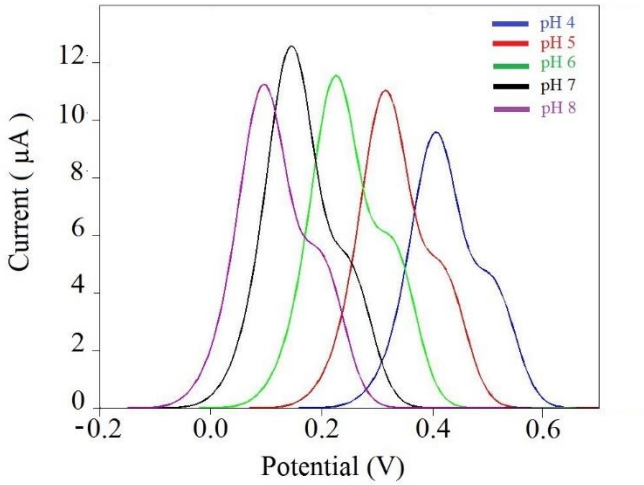

Figure 7. The differential pulse voltammograms of AA, DA and UA mixture (10^{-4} M) using the 3DG/CNT-SPE at different pH buffer solutions from 4 to 8

3.4 Electrochemical behavior of the analytes and multivariate calibration

The typical differential pulse voltammograms of individual and mixture of AA, DA, and UA are shown in Fig. 8a. Single component analysis for each of neurotransmitters was carried out using DPV technique. The relationship between peak current and concentration of each analyte was fitted in a linear model while other analytes were present in solution and at constant level. The oxidation peak currents increase with increasing concentration, which indicates the electrocatalytic behavior of 3DG/CNT-SPE. The voltammogram of the mixture shows overlapping peaks. In order to resolve the peaks, and improve the detection limit the PLS regression algorithm was applied to the data generated by the POC device. For simultaneous determination of the analytes, firstly, the calibration set was constructed using 30 standard mixture samples in the potential region from -0.1 to +0.7 V (Table S1). The second step is choosing number of significant factors to construct the model. The accuracy of the predicted results from unknown samples largely depends on the number of selected factor. To calculate the prediction error, the leave one out cross validation method was used. A new calibration is built with removing one sample from the calibration set. The removed data is used as test sample for new model. Each sample is left out

once and the process is repeated. The desirable number of factors are chosen when predictive residual sum of squares (PRESS) value is minimized. PRESS function is calculated using Eq. (1):

$$PRESS(k) = \sum_{n=1}^{sample} \left(C_i + \hat{C}_i\,(\mathrm{k})\right) \quad (1)$$

Where *k* is the number of factors, C_i is the real concentration of analyte, and $\hat{C}_i$ is the calculated concentration of i_{th} sample by multivariate calibration based on *k* factors. The calculations were repeated for each analyte. The obtained calibration model, with a determination coefficient (R^2) of 0.9970, was further validated with a test set of 10 mixture samples of the target analytes (Table 1) electrode. Most of the obtained recoveries were within the acceptable range of 97-102 %. The results show similar recoveries in both low and high concentration, which reveals that the calibration range is accurate and not affected by concentration. As can be seen, the method is capable of detecting each component in the presence of considerable amount of two others Figs. 8b-8d. The linear concentration range were 4-2000, 0.5-2000, and 0.8-1500 µM for DA, AA, and UA, respectively, and calculated detection limits are as follows AA (2.5 µM), DA (0.4 µM), and UA (0.6 µM).

Table 1. Testing 10 known standard samples with the developed POC device.

Standard	Standard (Concentration, µM)			Obtained (Concentration, µM)			Recovery (%)		
	AA	UA	DA	AA	UA	DA	AA	UA	DA
1	150	180	900	152	177	903	101	98.3	100
2	400	90	200	396	90	199	99	100	99.5
3	15	60	70	15	61	68	100	101	97.1
4	2000	500	120	1995	495	122	99.7	99	101
5	375	250	11	374	247	10	99.7	98.8	90
6	700	20	50	702	20	51	100	100	102
7	1200	60	550	1189	65	551	99	108	100
8	200	1000	30	200	1004	31	100	100	103
9	2000	1500	1500	1988	1496	1537	99.4	99.7	102.5
10	75	700	1200	76	698	1203	101	99.7	100

In order to test the repeatability of the electrode (n=15), the peak current for a ternary mixture of AA (2.5×10^{-4} M), DA (1.0×10^{-4} M) and UA (1.5×10^{-4} M) were recorded. The RSD were calculated as 3.5, 2.6 and 3.2% for AA, DA and UA, respectively which indicates the 3DG/CNT-SPE electrode is resistant to fouling. To test the reproducibility electrode to electrode, five 3DG/CNT-SPE were tested under the same experimental conditions and the RSDs were 1.5, 1.8 and 2.2 % for AA, DA and UA, respectively were recorded therefore, the fabricating process shows good reproducibility.

3.5 Real sample analysis

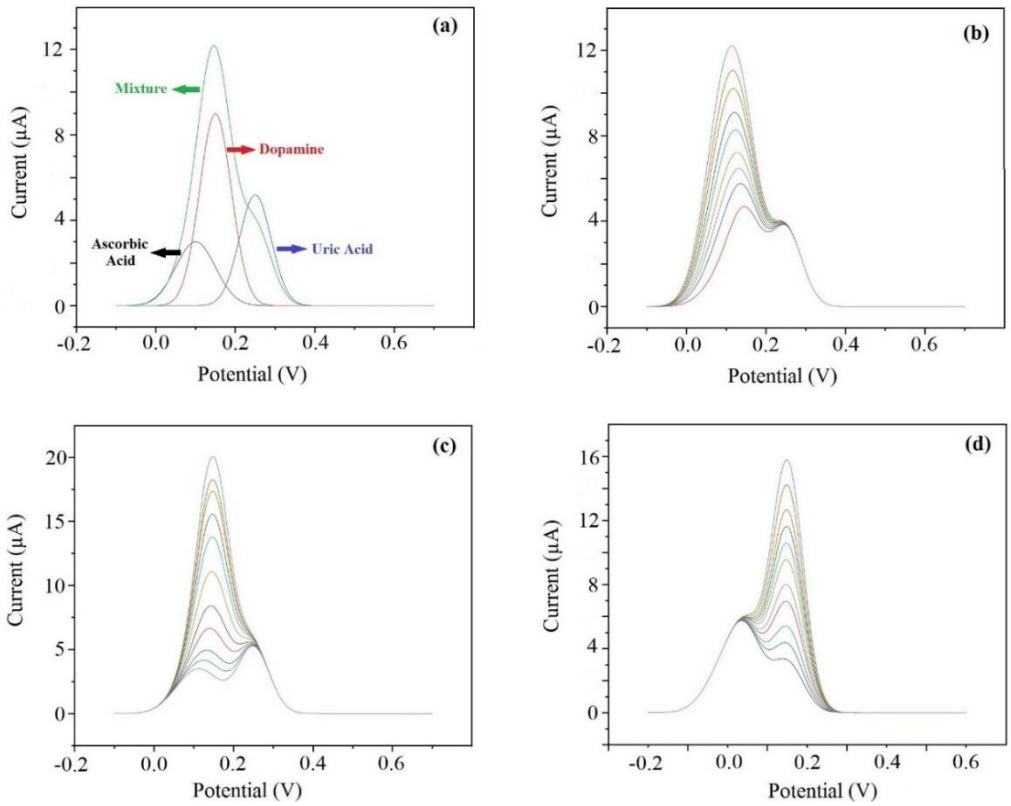

Figure 8 (a) The differential pulse voltammograms for dopamine, ascorbic acid, uric acid and mixture (10^{-4} M in PBS). (b) Differential pulse voltammograms of ascorbic acid (5×10^{-5} M to 3.5×10^{-4}) in presence of dopamine and uric acid at the modified 3DG/CNT-SPE electrode in 0.1 M PBS (pH 7). Step potential=2.5 mV. (c) Differential pulse voltammograms of dopamine (10^{-5} M to 2×10^{-4}) in the presence of ascorbic acid and uric acid at the modified 3DG/CNT-SPE electrode in 0.1 M PBS (pH 7). Step potential=2.5 mV. (d) Differential pulse voltammograms of uric acid (6×10^{-5} M to 3×10^{-4}) in the presence of dopamine and ascorbic acid at the modified 3DG/CNT-SPE electrode in 0.1 M PBS (pH 7). Step potential=2.5 mV.

The applicability of the developed method was evaluated with analysis of two plasmas and two urine real samples obtained from a local medical laboratory (Danesh Lab., Tehran, Iran). A six mL of the sample was placed in a vial and 7 mL of buffer solution mixing was added to it to adjust pH at ~7. Then, 3 mL MeOH was added to the solution and the mixture was centrifuged (3000 rpm) for 10 min. Finally, the samples were spiked with standard solutions of the analytes at different concentration levels. The unspiked and spiked real samples were analyzed with the POC device and the results were given in Table 2. The results show that satisfactory recoveries were obtained for AA (107-120 %), DA (82-110 %), and UA (93-110 %) that indicate the ability of 3DG/CNT-SPE modified electrode for determination of the target analytes in the real samples.

The developed method was compared with other published methods for determination of UA, DA, and AA and the results were summarized in Table 3. As it is obvious, the LODs are better than some and comparable to the others.

Table 2. Real samples analyzed with the developed POC analyzer.

Sample	Spiked (µM)			Found ±RSD %(µM) (n=3)		
	AA	UA	DA	AA	UA	DA
Plasma 1	200	50	30	215 (± 5.7)	41(± 3.3)	33(± 0.8)
Plasma 2	25	200	130	30 (± 1.2)	205(± 8.5)	121(± 4.4)
Urine 1	300	10	50	341(± 9.5)	11(± 0.7)	50(± 2.1)
Urine 2	40	20	180	43(±1.6)	19(±1.2)	173(± 7.8)

Table 3. Comparison of the proposed method with other methods.

Method	Electrode	Analyte	LDR [a]	LOD [b]	Ref.
SWV [c]	AuNPs-CD-G [d]	UA [e]	0.5-60	0.12	31
		DA [f]	0.5-150	0.15	
		AA [g]	30-2000	10	
DPV [h]	Trp-GR [i]	UA	10-1000	1.24	32
		DA	0.5-110	0.29	
		AA	0.2-12.9	10.29	
DPV	p-ATP modified GC [j]	UA	-	0.59	33
		DA	-	0.19	
		AA	-	2.01	
DPV	Fe3O4@Au-Cys/PANI/GFE [k]	UA	20-1000	1.8	34
		DA	20-1000	2.19	
		AA	-		
DPV	GN/PANI/Au [l]	UA	1400-2900	47	35
		DA	70-5240	24	
		AA	1550-9940	440	
SWV	SFO-GCE [m]	UA	0.3-10	0.05	36
		DA	0.5-20	0.09	
		AA	-	-	
DPV	SDS-MWCNTs [n]	UA	4.30	0.04	37
		DA	0.8-80	0.01	
		AA	400-3500	3	
DPV	3DG/CNT-SPE	UA	0.8-1500	0.6	This work
		DA	0.5-2000	0.4	
		AA	0.5-2000	2.5	

[a] Linear dynamic range (µM). [b] Limit of detection (µM). [c] Square wave voltammetry. [d] Gold nanoparticles-ß-cyclodextrin–graphene-modified electrode. [e] Uric acid. [f] Dopamine. [g] Ascorbic acid. [h] Differential pulse voltammetry. [i] Tryptophan-functionalized graphene nanocomposite. [j] 2-Amino-1,3,4-thiadiazole modified glassy carbon. [k] Gold-cysteine polyaniline graphite. [l] Graphene/polyaniline gold. [m] Poly Safranine O- Glassy carbon electrode. [n] Sodium dodecyl sulfate-multi-walled carbon nanotubes

The linearity of the method is better than that of the others. In addition, the capability for in-situ detection of AA, DA, and UA in biological samples is a main advantage of the developed method over the other methods.

4. CONCLUSIONS

A portable health monitoring device including a microcontroller-based potentiostat (MP), a designed syringe pump system in tandem with a microfluidic chamber and the MP was developed the first time. A 3DG/CNT-SPE modified electrode was successfully interfaced with the potentiostat for determination of dopamine (DA), ascorbic acid (AA), and uric acid (UA) in human plasma and urine samples. The modified electrode provided a broadly accessible surface and showed a remarkable increase in the kinetics of electron transfer rate. In addition, it decreased the overpotential for oxidation of the analytes and enhanced oxidation peak current. The PLS method techniques was utilized to resolve the overlapped peaks. The developed potentiostat is capable of detecting AA, DA, and UA at 2.5, 0.4, 0.6 μM levels with a linearity of 4-2000, 0.5-2000, and 0.8-1500 μM, respectively. The results were in good agreement with other similar commercial instruments suggest that the developed device could be used as a POC device to monitor the target analytes.

CONFLICTS OF INTEREST
There are no conflicts to declare.

References

1. L. Syedmoradi, M. Daneshpour, M. Alvandipour, F.A. Gomez, H. Hajghassem, and K. Omidfar, *Biosens. Bioelectron.*, 87 (2017) 373.
2. T. Tian, J. Li, Y. Song, L. Zhou, Z. Zhu, and C.J. Yang, *Lab Chip*, 16 (2016) 1139.
3. F. A. Gomez, *Bioanalysis,* 5 (2013) 1.
4. B. Srinivasan, and S. Tung, *J. Lab. Autom.*, 20 (2015) 365.
5. S. Alwarappan, G. Liu, and C.Z. Li, *Nanomed.-Nanotechnol.*, 6 (2010) 52.
6. Y.J. Yang, and W. Li, *Biosens. Bioelectron.*, 56 (2014) 300.
7. W. Zhang, R. Yuan, Y.Q. Chai, Y. Zhang and S.H. Chen, *Sens. Actuators, B*, 166–167 (2012) 601.
8. R.N. Adams, *Anal. Chem.*, 48 (1976) 1126A.
9. L. Lin, J. Chen, H. Yao, Y. Chen, Y. Zheng, and X. Lin, *Bioelectrochemistry*, 73 (2008) 11.
10. H. Zhang, P. Gai, R. Cheng, L. Wu, X. Zhang, and J. Chen, *Anal. Methods*, 5 (2013) 3591.
11. M. Noroozifar, M. Khorasani-Motlagh, R. Akbari, and M. Bemanadi Parizi, *Biosens. Bioelectron.*, 28 (2011) 56.
12. M. Zhou, Y. Zhai and S. Dong, *Anal. Chem.*, 81 (2009) 5603.
13. C.L. Sun, H.H. Lee, J.M. Yang, and C.C. Wu, *Biosens. Bioelectron.*, 26 (2011) 3450.
14. S. Wang, W. Zhang, X. Zhong, Y. Chai, and R. Yuan, *Anal. Methods*, 7 (2015) 1471.
15. S. Mahpishanian, and H. Sereshti, *J. Chromatogr. A*, 1443 (2016) 43.
16. D.C. Marcano, D.V. Kosynkin, J.M. Berlin, A. Sinitskii, Z. Sun, A. Slesarev, L.B. Alemany, W. Lu, and J.M. Tour, *ACS nano,* 4 (2010) 4806.
17. Z. Chen, W. Ren, L. Gao, B. Liu, S. Pei, and H.M. Cheng, *Nat. Mater.*, 10 (2011) 424.
18. Y. Xu, K. Sheng, C. Li, and G. Shi, *ACS nano,* 4 (2010) 4324.

19. H. Bai, C. Li, X. Wang, and G. Shi, *J. Phys. Chem.*, 115 (2011) 5545.
20. K. Chen, L. Chen, Y. Chen, H. Bai, and L. Li, *J. Mater. Chem.*, 22 (2012) 20968
21. S. Wold, M. Sjöström, and L. Eriksson, *Chemom. Intell. Lab. Syst.*, 58 (2001) 109.
22. R. Jadon, R. Jain, S. Sharma, and K. Simgh, *Talanta*, 161 (2016) 894.
23. Y. Ni, Y. Gui, and S.Kokot, *Anal. Methods*, 3 (2011) 385.
24. Y. Ni, P, Qui, and S. Kokot, *Anal. Chim. Acta*, 516 (2004) 7.
25. Y. Ni, L. Wang, and S. Kokot, *Anal. Chim. Acta*, 431 (2001) 101.
26. M. Hilal, and J.I. Han, *Sol. Ener*., 174 (2018) 743.
27. Z. Chen, W. Ren, L. Gao, B. Liu, S. Pei, and H.M. Cheng, *Mater. Lett.*, 10 (2011) 424.
28. M. Mallesha, R. Manjunatha, V. Nethravathi, G.S. Suresh, M. Rajamathi, J.S. Melo, and T.V. Venekatesha, *Bioelectrochemistry,* 81(2011) 104
29. Z. Monsef Khoshhesab, *RSC Adv*., 115 (2015) 95140.
30. Y. Yang, and L.L. Tong, *Sens. Actuators, B*, 150 (2010) 43.
31. X. Tian, C. Cheng, H. Yuan, J. Du, D. Xiao, S. Xie, and M.M. Choi, *Talanta*, 93 (2012) 79.
32. Q. Lian, Z. He, Q. He, A. Luo, K. Yan, D. Zhang, X. Lu, and X. Zhou, *Analytica chimica acta*, 823 (2014) 32.
33. P. Kalimuthu, and S.A. John, *Talanta*, 80 (2010) 1686.
34. N. Nontawong, M. Amatatongchai, W. Wuepchaiyaphum, S. Chairam,S. Pimmongkol, S. Panich, S. Tamuang and P. Jarujamrus, *Int. J. Electrochem. Sci.,* 13 (2018) 6940.
35. L. Shi, Z. Wang, G. Gou, X. Chen, G. Yang and W. Liu, *Int. J. Electrochem. Sci.,* 12 (2017) 2540.
36. H. Filik, A. Aslihan Avan, S. Aydar and R. Bozdogan *Int. J. Electrochem. Sci.,* 9 (2014) 2775.
37. J. Zhang, Z. Zhu, J. Zhu, K. Li and S. Hua *Int. J. Electrochem. Sci.,* 9 (2014) 1264.